ACS central science

Research Article

Cite This: ACS Cent. Sci. 2019, 5, 629−639

http://pubs.acs.org/journal/acscii

# Redirecting Pore Assembly of Staphylococcal α-Hemolysin by Protein Engineering

Sunwoo Koo,*[,†] Stephen Cheley,[‡,∥] and Hagan Bayley*[,§]

[†]Department of Neuroscience and Experimental Therapeutics, Texas A&M University Health Science Center, 8447 Riverside Parkway, Bryan, Texas 77807, United States

[‡]Department of Pharmacology, Alberta Diabetes Institute, University of Alberta, Edmonton, T6G 2E1 Alberta, Canada

[§]Department of Chemistry, University of Oxford, Chemistry Research Laboratory, Mansfield Road, Oxford, OX1 3TA England, United Kingdom

Supporting Information

**ABSTRACT:** α-Hemolysin (αHL), a β-barrel pore-forming toxin (βPFT), is secreted as a water-soluble monomer by *Staphylococcus aureus*. Upon binding to receptors on target cell membranes, αHL assembles to form heptameric membrane-spanning pores. We have previously engineered αHL to create a protease-activatable toxin that is activated by site-specific proteolysis including by tumor proteases. In this study, we redesigned αHL so that it requires 2-fold activation on target cells through (i) binding to specific receptors, and (ii) extracellular proteolytic cleavage. To assess our strategy, we constructed a fusion protein of αHL with galectin-1 (αHLG1, αHL-Galectin-1 chimera). αHLG1 was cytolytic toward cells that lack a receptor for wild-type αHL. We then constructed protease-activatable mutants of αHLG1 (PAMαHLG1s). PAMαHLG1s were activated by matrix metalloproteinase 2 (MMP-2) and had approximately 50-fold higher cytolytic activity toward MMP-2 overexpressing cells (HT-1080 cells) than toward non-overexpressing cells (HL-60 cells). Our approach provides a novel strategy for tailoring pore-forming toxins for therapeutic applications.

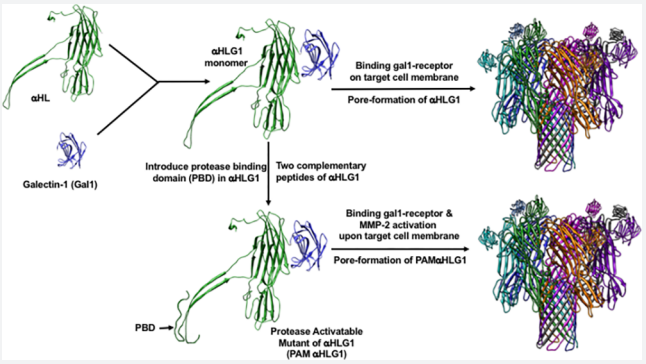


Engineered pore-forming toxins (PFTs) have been extensively studied and applied in biotechnology.[1,2] A few PFTs have been successfully employed in the field of biomolecule sensing, such as DNA sequencing.[2] The structures and assembly mechanisms of PFTs, knowledge of which is essential for efficient protein engineering, have been thoroughly studied: β-barrel pore-forming toxins (βPFTs), such as aerolysin,[3] anthrax toxin,[4] *Vibrio cholerae* cytolysin (VCC),[5] and α-hemolysin (αHL),[6] which form membrane-spanning β-barrels, bind to specific cell-surface receptors, assemble into inactive prepore intermediates, and transform into membrane-spanning active pores.[7] Among these βPFTs, aerolysin,[8] anthrax toxin[9] and VCC,[10] for example, are synthesized as inactive forms of toxin called "prolysins" and require proteolytic cleavage of redundant a peptide at the C-terminus or N-terminus to generate cytolytic activity toward target cells by receptor binding and pore-formation.[11] For example, furin activates proaerolysin[8] and proanthrax toxin[9] by cleaving peptides from the C-terminus and N-terminus, respectively, and A Disintegrin and Metalloprotease 17 (ADAM-17) activates pro-VCC by cleaving peptides from the N-terminus,[10] presumably after binding to the receptor on target cell membranes.[5] The proteolytic activation of prolysin is an important requirement in the assembly of a toxin, the absence of which prevents the assembly of lytic pores into nontarget membranes. The 2-fold action of receptor binding and protease activation enhances cell specificity. In the present work, we introduce such a 2-fold specificity into αHL by protein engineering.

Protein redesign using genetic modification provides a tuning strategy for the alteration of toxin properties without eliminating cytotoxicity.[1] Several studies have constructed PFT fusion proteins with target-specific ligands such as a colicin−pheromone fusion protein targeted to *Staphylococcus aureus*.[12] Mechaly et al. constructed an anthrax−EGFR fusion protein, and ablated the native receptor-binding domain of anthrax toxin to improve the receptor specificity toward targeted EGFR bearing cells.[13] In addition to specific receptor binding, proteolytic cleavage to activate a prolysin provides a highly effective tool for the development of 2-fold specificity. Anthrax toxins have been re-engineered by swapping the furin-recognition domain (i.e., a native protease-recognition domain) with matrix metalloprotease-recognition (MMP-recognition) domain and have shown selective toxicity to MMP overexpressing tumor cells.[14,15] The requirement for the

**Received:** December 7, 2018
**Published:** March 25, 2019




DOI: 10.1021/acscentsci.8b00910
ACS Cent. Sci. 2019, 5, 629−639

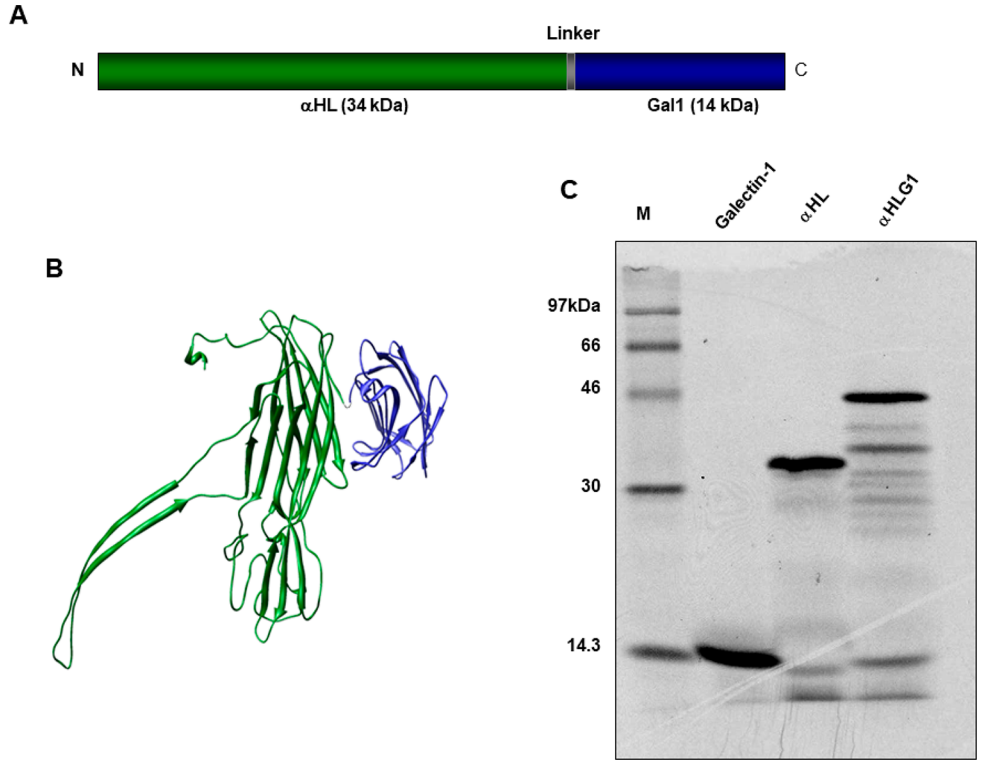


**Figure 1.** Construction of αHLG1. (A) αHLG1 comprises human galectin-1 (Gal1, 14 kDa) fused to the C-terminus of staphylococcal α-hemolysin (αHL, 34 kDa) through a linker (TSSGSS). (B) Representation of the αHLG1 monomer. (C) Expression of monomeric forms of galectin-1, αHL, and αHLG1. The proteins were synthesized by IVTT (In Vitro Transcription and Translation) in the presence of [$^{35}$S]methionine and subjected to electrophoresis in a 10% SDS-polyacrylamide gel followed by autoradiography. The molecular masses of galectin-1, αHL, and αHLG1 are 14, 34, and 48 kDa, respectively. M: protein molecular mass markers ([$^{14}$C]methylated protein, Amersham Bioscience).

activation of certain PFTs on the target cell membrane provides a strategy for tailoring cytolytic activity dependent on a specific protease secreted from target cells. In addition to redirecting toxins by the fusion of a heterologous ligand, this ability to regulate cytotoxicity by redesign will greatly contribute to increased cell target specificity.

Pore assembly mechanisms of αHL and its distinct pore properties have been studied using biochemical and genetic approaches.[16−18] αHL lyses rabbit erythrocytes at concentrations 1000-fold lower than those required for human erythrocytes.[19] αHL has been shown to bind to target cell membranes via direct interactions with specific membrane lipids and binding to specific receptors, such as phosphocholine headgroups[20,21] and A Disintegrin and Metalloprotease 10 (ADAM 10).[22] These results account for the high αHL cytolytic activity toward rabbit erythrocytes, which express ADAM 10 highly by comparison with human erythrocytes.[22] To closely explore the mechanism of pore assembly, we previously identified important domains in the αHL polypeptides for binding, oligomerization, and pore formation by using 83 single-cysteine point mutagenesis and truncation mutagenesis.[6,17]

We previously constructed a complementation mutant of αHL consisting of two truncated polypeptide segments encompassing the N-terminal and C-terminal halves of the polypeptide chain. This discontinuous αHL mutant with a nick in the stem domain demonstrated that the integrity of the stem domain of αHL is not required for pore-formation.[23] Based on this knowledge, we engineered αHL by introducing redundant peptides containing protease recognition sites in discountinuous stem domains. These toxins remained inactive unless the redundant peptides were removed by site-specific proteases[24] such as cathepsin B (i.e., a tumor protease).[25] This was the first reported approach that exogenously introduced a protease-recognition site as a "protease-actuated trigger" in the core region of the pore-formation component of a PFT that does not have a native protease-binding domain.

In this study, we redesigned a complementation mutant of αHL by introducing a tumor protease-recognition site in the stem domain and a receptor-binding domain (i.e., αHL-lectin chimera) at the C-terminus. This mutant required 2-fold activation to produce cytolytic activity toward target cells. The design of this toxin−lectin chimera was based on the characteristics of *Vibrio cholera* cytolysin (VCC), which has high structural similarity to αHL, but contains two additional C-terminal lectin domains that take part in cell binding and pore-formation: a β-prism domain that interacts with carbohydrate receptors on cell membranes,[26] and a β-trefoil domain that may be involved in oligomerization.[5] Additionally, VCC contains a protease-recognition site that enables the proteolytic cleavage of the proregion that results in conversion of pro-VCC to mature VCC.[5,10] To assess the feasibility of our approach, we constructed a protease-activatable mutant of αHLG1 (PAMαHLG1). We fused galectin-1 to the C-terminus of αHL (αHLG1). We then introduced a protease-recognition site in the stem loop of αHLG1 flanked by a peptide extension so as to inactivate the toxin (i.e., form a prolysin). Our approach provides a template for engineering PFTs for therapeutic applications.



DOI: 10.1021/acscentsci.8b00910
*ACS Cent. Sci.* 2019, 5, 629−639

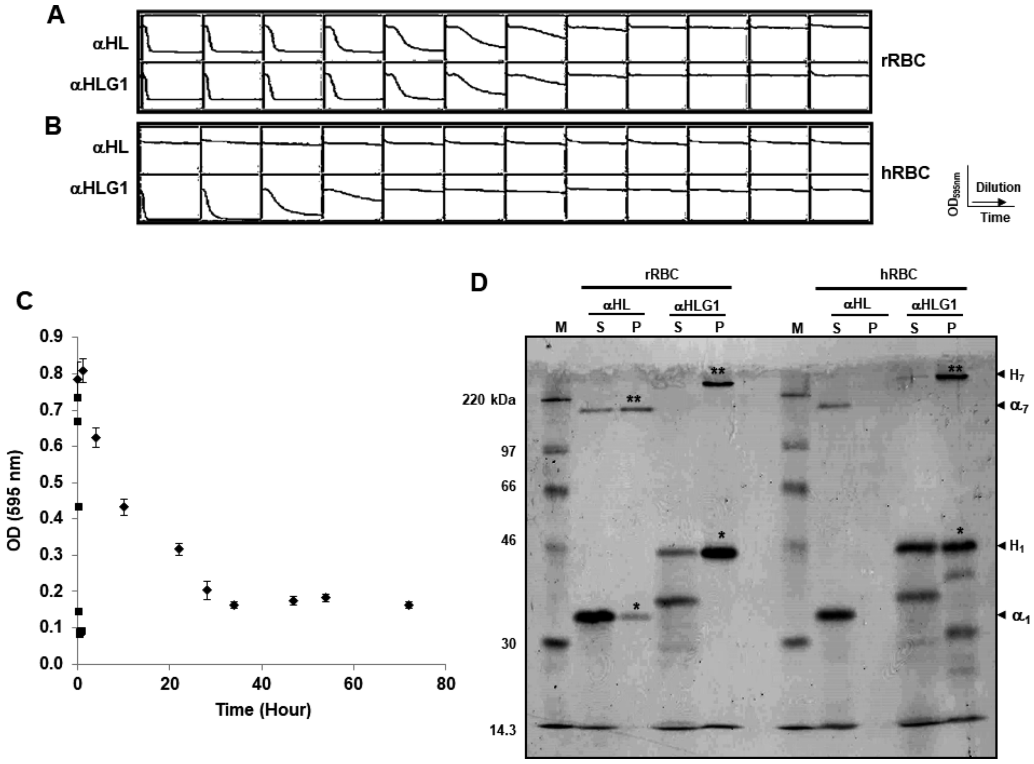


**Figure 2.** Hemolytic activities of αHL and αHLG1 toward rabbit and human erythrocytes. IVTT proteins (29 nM) were added to the first well of each row in a microtiter plate and subjected to 2-fold serial dilution in MBSA across each row leaving 50 μL in each well. 1.0% rRBCs (A) or hRBCs (B) suspended in MBSA (50 μL) were then added to each well (0.5% final concentration of RBCs), and the light scattering at 595 nm was recorded over 2 h. (C) Long-duration hemolytic activity assays for αHL and αHLG1 toward hRBCs. The activities of αHL (◆) and αHLG1 (■) (48 nM) toward hRBC were monitored for 72 h. The results plotted are from three independent assays (mean ± SD, $n$ = 3). (D) Extents of binding of αHL and αHLG1 to RBC as demonstrated by SDS-polyacrylamide gel electrophoresis. IVTT proteins (29 nM) were incubated with 0.5% rRBC (left) or 0.5% hRBC (right) for 20 min at room temperature. * membrane-bound monomer; **, membrane-bound heptamer. M: Protein molecular mass markers, $^{14}$C-methylated protein (Amersham Bioscience). $H_1$, αHLG1 monomer; $\alpha_1$, αHL monomer; $H_7$, αHLG1 heptamer; $\alpha_7$, αHL heptamer.

## RESULTS

**αHLG1 Has Increased Hemolytic Activity toward Human RBCs Compared with αHL.** Engineered αHLs with C-terminal extensions have been previously reported to form functional pores. For example, αHL fused to the 94 amino acid residues (289−382) of the C-terminal tail of hemolysin II from *Bacillus cereus*[27] and subunit dimers of αHL (αHL-linker-αHL)[28] are hemolytically active. In the present study, we fused galectin-1 (14 kDa) to the C-terminus of αHL (34 kDa) through a glycine−serine linker (TSSGSS) to form αHLG1 (48 kDa) (Figure 1A−C). The fused lectin domain (galectin-1) was introduced by cassette mutagenesis, and is readily switchable to other binding molecules, such as mAbs and cancer-specific ligands. Galectin-1 is a β-galactoside-binding protein with high affinity toward human erythrocytes.[29] αHLG1 (29 nM) exhibited the same hemolytic activity toward 0.5% rabbit red blood cells (rRBCs) as αHL (wild-type αHL, 29 nM) (Figure 2A). By contrast, αHLG1 bound more extensively to human red blood cells (hRBCs) and had a higher hemolytic activity toward hRBCs compared with αHL (wild-type αHL) (Figure 2B,D). We assessed the differential hemolytic activity between αHLG1 and αHL toward hRBCs through long-duration hemolysis assays. αHLG1 exhibited a 172-fold higher lysis rate (% cell lysiss $^{-1}$) (Figure 2C and Table 1, % cell lysis = $((OD_{initial} - OD_{80})/(OD_{initial} - OD_{final})) \times 100$, where $OD_{initial}$, $OD_{final}$, and $OD_{80}$ are OD values (595 nm) at initial, final, and 80% cell lysis timepoints, respectively). The initial lag period (time to 10% lysis) of αHLG1 was 21 times shorter than that of αHL on hRBC (Figure 2C and Table 1). αHLG1 formed SDS-stable oligomers on both rRBCs and hRBCs, whereas αHL did so only on rRBCs, as analyzed by SDS-polyacrylamide gel electrophoresis (Figure 2D). The extents of binding of αHLG1 to both rRBCs and hRBCs were higher than those of αHL: 2-fold higher for rRBCs and 1000-fold higher for hRBCs (Table S1). Galectin-1 has been reported to increase the osmofragility of hRBCs by cross-linking membrane constituents.[29,30] We found that galectin-1 itself had no such effect (Figure S2). We concluded that the binding of galectin-1 to hRBC membranes improved the hemolytic activity of αHLG1.

**Table 1. Hemolytic Activity Comparison Chart**

| | initial lag period (s) | lysis rate (% cell lyseds $^{-1}$) |
|---|---|---|
| αHL | 2500 | $6.2 \times 10^{-6}$ |
| αHLG1 | 120 | $1 \times 10^{-3}$ |

**Inhibition of αHLG1 Binding to hRBCs by Carbohydrates.** To verify the role of the galectin-1 domain in the binding of αHLG1 to hRBCs, we performed an inhibition assay. Lactose is a well-known inhibitor of galectin-1,[30] and it has been reported that more than 10 mM lactose is required to efficiently inhibit galectin-1 activity.[31] We performed an inhibition assay with various concentrations of lactose and


DOI: 10.1021/acscentsci.8b00910
ACS Cent. Sci. 2019, 5, 629−639

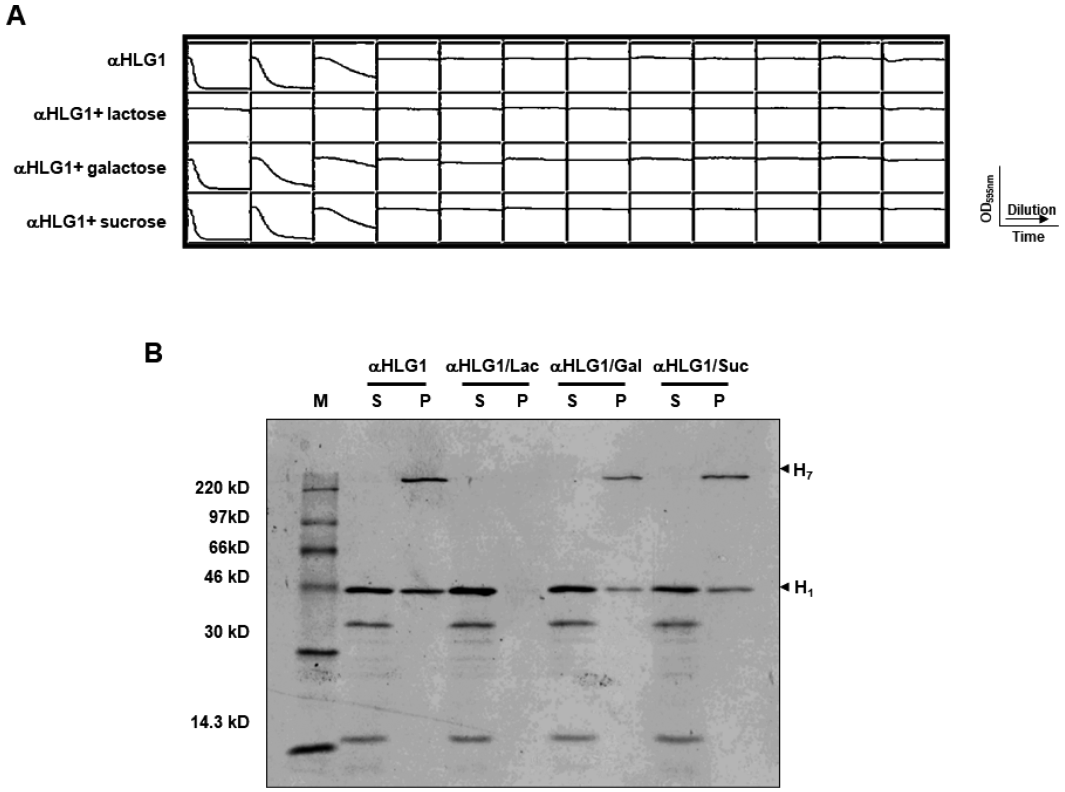


**Figure 3.** Inhibition of αHLG1 activity toward hRBCs by carbohydrates. (A) Inhibition of the hemolytic activity of αHLG1 toward hRBCs. αHLG1 preincubated (20 min) with carbohydrates (lactose, galactose, sucrose: 10 mM) was added to the first well of each row and 2-fold serially diluted across the row (50 μL final volume in each well). The hemolysis assay was initiated by adding 1% hRBCs (50 μL to each well, 0.5% RBCs final). (B) Inhibition of binding and oligomerization. αHLG1 (20 nM), which had been preincubated with a carbohydrate (10 mM), was incubated with 0.5% hRBCs for 20 min at room temperature. A membrane pellet was recovered by centrifugation and resuspended in MBSA. The pellets and supernatants (αHLG1, αHLG1/lactose, αHLG1/galactose, αHLG1/sucrose) were examined by electrophoresis in a 10% SDS-polyacrylamide gel, followed by autoradiography. M, protein molecular mass markers; Lac, lactose; Gal, galactose; Suc, sucrose.

found that 10 mM lactose completely inhibited the hemolytic activity of αHLG1 (20 nM) (Figure 3A) and diminished the binding of αHLG1 toward hRBCs (Figure 3B) while 3 and 6 mM lactose partially inhibited the hemolytic activity (Figure S3). By contrast, galactose and sucrose failed to completely inhibit both the binding and hemolysis of αHLG1 toward hRBCs (Figure 3A,B). These results suggest that the galectin-1 domain of αHLG1 binds to the surfaces of hRBCs and facilitates the hemolysis by the αHL domain of αHLG1.

**Cytotoxicity of αHLG1 toward Cancer Cells Is Higher than That of αHL.** We assessed whether the galectin-1 domain of αHLG1 mediated binding to human cancer cells (HL-60, promyelocytic leukemia) expressing galectin-1 receptors as it does toward RBCs. Both monomeric and dimeric galectin-1 have been reported to bind to HL-60 cells through poly-*N*-acetyllactosamine (Galβ1−4GlcNAc).[30] We evaluated the cytolytic activity of αHLG1 toward HL-60 cells using flow cytometry (Figure 4A and Figure S5). In brief, lysed cells and healthy cells (10 000 cells in total) were sorted and quantified using two parameters: forward-scattered light (FSC, proportional to cell-surface size) and side-scattered light (SCC, proportional to cell granularity). The cytolytic activity of αHLG1 (19 nM) was at least 2-fold higher than that of αHL (19 nM) toward HL-60 cells ($1 \times 10^7$ cells $mL^{-1}$, Figure 4A). αHLG1 also had a shorter lag period (time to 5% cell death): αHLG1, 25 min; αHL, 35 min. The percentages of cell death at 45 min were 10.0 ± 0.5% for αHL and 24.6 ± 2.6% for αHLG1 (mean ± SD, $n = 3$), and the lysis rates (% cell death $min^{-1}$) were 0.38 ± 0.01 for αHL and 0.78 ± 0.04 for αHLG1 (mean ± SD, $n = 3$). These findings were consistent with the results of quantitative binding assays (αHL, 9.6% of αHL bound; αHLG1, 43% of αHL bound) (Figure 4B and Table S1).

We evaluated the binding and cytolytic activity of αHLG1 on different cell types (other than RBCs and HL-60 cells), e.g., human fibrosarcoma cells (HT-1080 cells, $1 \times 10^7$ cells $mL^{-1}$). HT-1080 cells display *N*-acetyllactosamine, a receptor for galectin-1,[32] and express matrix metalloproteinases (MMPs), which are required for activation of PAMαHLG1.[33] αHLG1 (48 nM) had cytolytic activity toward HT-1080 cells (69%), which was higher than that of αHL (28%) (Figure 4C). αHLG1 formed SDS-stable oligomers in the presence of HT-1080 cells, whereas αHL monomers were detected, but oligomers were not (Figure 4D). Based on a band intensity comparison, the extents of binding of αHLG1 and αHL (monomers and oligomers) to HT-1080 cell membranes were 42% and 13% of αHL bound, respectively (Table S1).

The cytotoxicities of αHLG1 toward cells from both a hematological malignancy (HL-60 cells) and a solid tumor (HT-1080 cells) were greater than that of αHL (Figure 4A,C). Our results suggest that αHL fusion protein with interchangeable receptor-binding domains may be readily modified and redirected to bind to targeted cells.

**Construction of PAMαHLG1, a Protease-Activatable Mutant of αHLG1.** PAMαHL, the two-chain overlap mutant of αHL, was prepared as previously described.[25] Two-chain


DOI: 10.1021/acscentsci.8b00910
ACS Cent. Sci. 2019, 5, 629−639

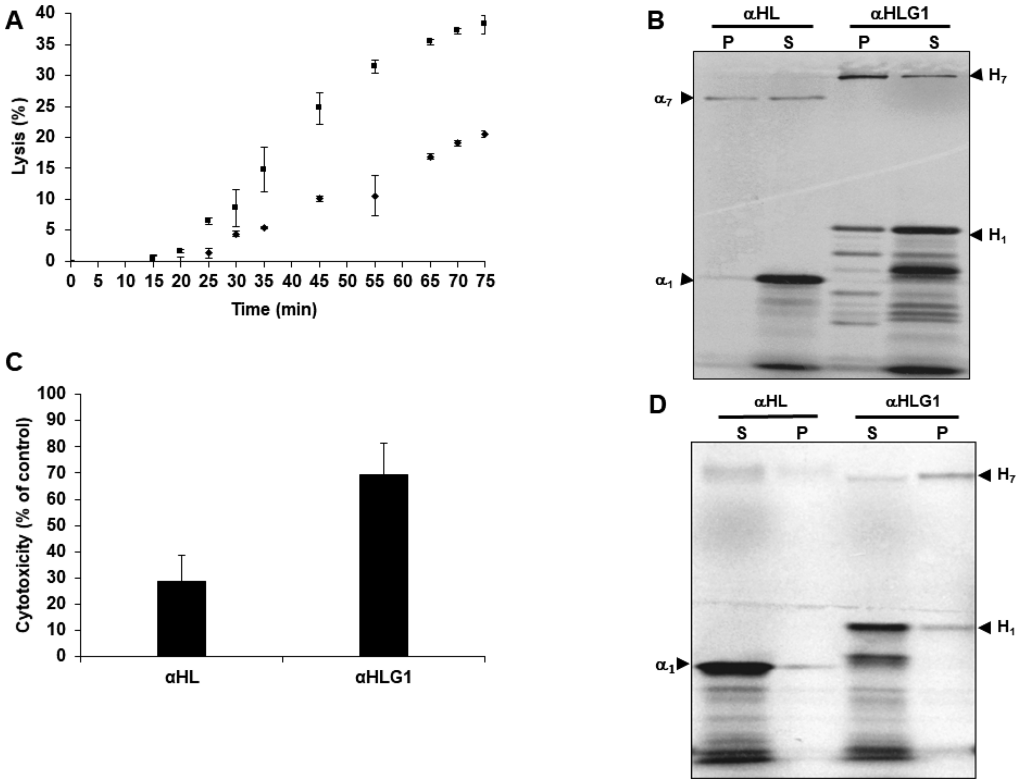


**Figure 4.** Cytotoxicity of αHLG1 toward human cancer cells. (A) Lysis of HL-60 cells as detected by flow cytometry. Lysis was monitored every 5 min for 75 min (10 000 cells at each time point) at room temperature: αHL (◆) and αHLG1 (■). Briefly, HL-60 cells were washed with PBS and medium (IMDM) containing 3% FBS. The assay was started by adding IVTT proteins (19 nM) to the cells ($1 \times 10^7$ cells $mL^{-1}$). % Lysis = (number of toxin-treated dead cells − number of untreated dead cells)/(10 000 − number of untreated dead cells) × 100. The detailed experimental procedures are described in Methods. (B) Extent of binding of αHL and αHLG1 to HL-60 cells in IMDM as determined by electrophoresis in a 10% SDS-polyacrylamide gel. Proteins (19 nM) radiolabeled with [$^{35}$S]methionine were incubated with cells ($1 \times 10^7$ cells $mL^{-1}$) for 40 min at room temperature. After centrifugation, the pellets were treated with DNase, and samples were subjected to 10% SDS-PAGE, followed by autoradiography: $\alpha_1$ and $H_1$, monomers of αHL and αHLG1, respectively; $\alpha_7$ and $H_7$, heptamers of αHL and αHLG1, respectively. (C) Cytotoxicity of αHL and αHLG1 toward HT-1080 cells. Protein (48 nM) was incubated with HT-1080 cells ($1 \times 10^7$ cells $mL^{-1}$) in assay medium (DMEM, 3% FBS) for 2 h with 5% $CO_2$ at 37 °C. The CytoTox 96 assay (Promega) was used to measure cytotoxicity. (D) Extent of binding of αHL and αHLG1 to HT-1080 cells. The toxins (48 nM) were incubated with HT-1080 cells in DMEM for 40 min at room temperature. Extents of binding were determined by electrophoresis in a 10% SDS-polyacrylamide gel, followed by autoradiography: $\alpha_1$ and $H_1$, monomers of αHL and αHLG1, respectively; $\alpha_7$ and $H_7$, heptamers of αHL and αHLG1, respectively.

overlap mutants of αHL are activated when redundant amino acids in the stem domain (β-barrels) are removed by proteolysis.[24] In other words, additional overlapping amino acid residues in the β-barrels of two-chain mutants of αHL inhibit cytolytic pore-formation. We have also demonstrated that few PAMαHLs selected from a library of candidates are activated by tumor proteases.[25] These results prompted us to construct PAMαHLG1s (protease-activatable mutants of αHLG1) by converting αHLG1 to a two-chain overlap mutant (Figure 5A). PAMαHLG1s are "prolysins" that require activation and incorporate a targeting mechanism conferring 2-fold specificity: (1) a galectin-1 domain to bind to receptors on the target-cell surface; and (2) a protease-recognition site for activation by removal of residues 119−132 (Figure 5A and Table S2). In this study, we constructed two mutants of αHL, PAMαHL (as a control) and PAMαHLG1: PAMαHL is composed of two truncated fragments of αHL, amino acids 1−131, 16 kDa, and amino acids 119−293, 22 kDa. PAMαHLG1 is composed of two truncated fragments of αHLG1: amino acids 1−131 and amino acids 119−293-galectin-1 of αHLG1, 36 kDa (Figure 5A,B).

**Cell-Specific Lytic Activity of PAMαHLG1.** The proteases, cathepsin B and matrix metalloproteinases (MMPs), are involved in tumor invasion and metastasis.[34,35] We constructed four different PAMs (protease-activatable mutants): PLHL and IGHL for PAMαHL, and PLHLG1 and IGHLG1 for PAMαHLG1. These proteins have two different MMP-recognition sequences: ···PLGLAGGG··· and ···TRRIGGLG···, which are prefixed PL- and IG-, respectively (Table S2). PXX↓$H_y$ ($H_y$, hydrophobic residue) is a good recognition motif for most MMPs, whereas L/IXX↓$H_y$, $H_y$SX↓L, and HXX↓$H_y$ are specifically recognized by MMP-2.[36] Therefore, PLHLG1 (PLG↓$H_y$) and IGHLG1 (L/IGG↓$H_y$) were evaluated for their ability to lyse hRBC after treatment with MMP-2 (0.3 μg $\mu L^{-1}$) (Figure 5C). Both constructs were activated for hemolysis by MMP-2, although the activity of IGHLG1 was higher than that of PLHLG1. PLHLG1 (36 nM) was also activated by cathepsin B (0.8 μg $\mu L^{-1}$) although its activity was limited, but IGHLG1 (36 nM) was not activated (Figure 5C). These findings were consistent with our previous report showing that αHL-RR (a two-chain mutant of αHL with the same protease-recognition site as IGHL/IGHLG1, Table S2) was not activated by cathepsin B.[25]

HT-1080 cells constitutively secrete MMP-2[33,37] and cathepsin B[38] and display *N*-acetyllactosamine, a galectin-1 receptor,[32] whereas HL-60 cells display *N*-acetyllactosamine


DOI: 10.1021/acscentsci.8b00910
ACS Cent. Sci. 2019, 5, 629−639

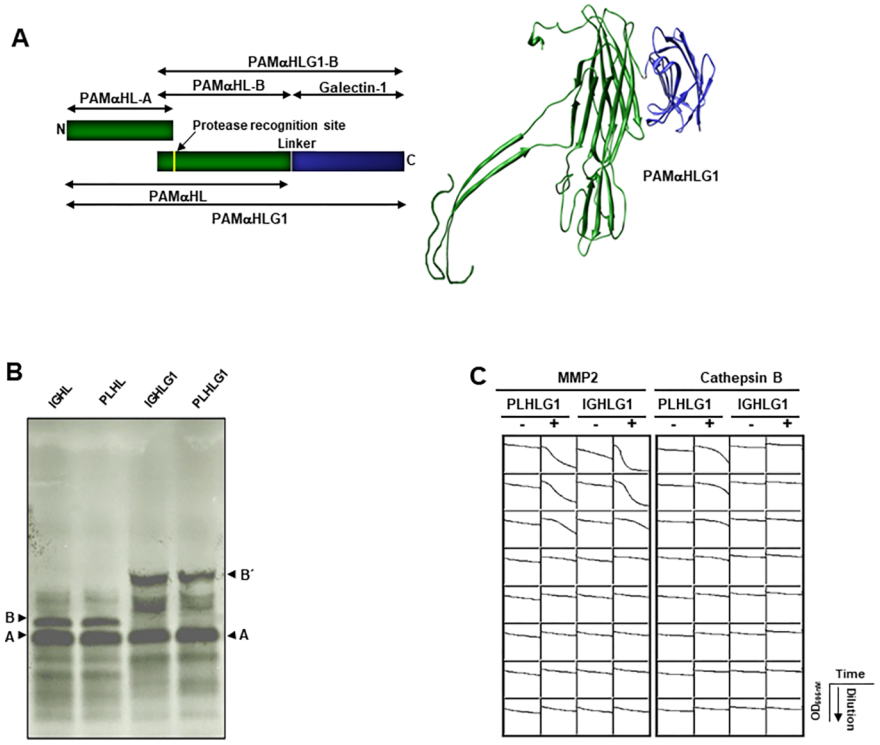


**Figure 5.** Protease-activatable mutants (PAMs) of $\alpha$-hemolysin. (A) Schematic diagram of PAMs. The proteins are composed of two polypeptide chains: PAM-A contains amino acids 1−131 of $\alpha$HL (16 kDa) and is present in both PAM$\alpha$HL and PAM$\alpha$HLG1. PAM$\alpha$HL-B is present in PAM$\alpha$HL and contains amino acids 119−293 of $\alpha$HL (22 kDa). PAM$\alpha$HLG1-B is present in PAM$\alpha$HLG1 and contains amino acids 119−293 of $\alpha$HL followed by a linker (TSSGSS) and galectin-1 (14 kDa). A protease recognition site is present in amino acids 127−134 of $\alpha$HL in both PAM$\alpha$HL-B and PAM$\alpha$HLG1-B. (B) Monomers of the PAMs were subjected to electrophoresis in a 10% SDS-polyacrylamide gel, followed by autoradiography. A, PAM-A; B, PAM$\alpha$HL; B′, PAM$\alpha$HLG1-B. (C) Hemolysis of hRBCs by PAM$\alpha$HLG1s after protease-activation. Activated PAM$\alpha$HLG1 was added to a well of a microtiter plate and subjected to 2-fold serial dilution in MBSA down a column of the plate to give a final volume of 50 $\mu$L in each well. Hemolysis assays were initiated by adding 1% hRBCs (50 $\mu$L) to the wells and monitored for 3 h by observing the decrease in light scattering at 595 nm. +, protease-treated hRBC; −, untreated hRBC.

and secrete cathepsin B[39] but do not overexpress MMP-2.[33,40] Accordingly, the susceptibility of HT-1080 cells to PAMs (PLHL, 9.8%; PLHLG1, 25%; IGHL, 8.0%; and IGHLG1, 19%) was higher than that of HL-60 cells (PLHL, 0.20%; PLHLG1, 1.9%; IGHL, 0.47%; and IGHLG1, 0.44%), suggesting that MMP-2 activated cytotoxicity (Figure 6A). Additionally, the cytotoxicity of PAM$\alpha$HLG1 (PLHLG1, 25%; and IGHLG1, 19%) was higher than that of PAM$\alpha$HL (PLHL, 9.8%; and IGHL, 8.1%) toward HT-1080 cells, suggesting that the galectin-1 domain of PAM$\alpha$HLG1 enhances activity (Figure 6A). Oligomers of PAM$\alpha$HLG1 associated with HT-1080 cells were visible on SDS-polyacrylamide gels, but PAM$\alpha$HL oligomers were not detected, while PAMs were cytotoxic (Figure 6B). No oligomers were detected on HL-60 cells (Figure 6B). To assess MMP-2 activity in our experimental model, we performed gelatin zymography using a 10% SDS-PAGE gelatin zymogram gel (Bio-Rad). Pro-MMP-2 (74 kDa) and active-MMP-2 (63 kDa) were detected in HT-1080 cells, but not in HL-60 cells (Figure 6C). This result clearly indicates that MMP-2 secreted from HT-1080 cells activates PAM$\alpha$HLG1s. Further, the dual regulatory domains of cytotoxicity in PAM$\alpha$HLG1, i.e., the fused galectin-1 domain and the MMP-2-recognition domain, did not eliminate the native cytolytic activity of $\alpha$HL. This result provides promising evidence of 2-fold specificity of engineered $\alpha$HL as we previously proposed.[41]

## DISCUSSION

In the present study, our approach was to modulate the cytotoxicity of $\alpha$HL by protein engineering. We re-engineered $\alpha$-HL into a protoxin chimera (PAM$\alpha$HLG1): Full length $\alpha$HL was fused with galectin-1, and divided into two complementary fragments, which are cotranslated in vitro. PAM$\alpha$HLG1 consists of three domains: the toxin domain ($\alpha$HL), a proteinase-recognition domain in the stem forming region of $\alpha$HL (MMP-2), and a receptor-binding domain at the C-terminus of $\alpha$HL (galectin-1) (Figure 5). Our future goal is to expand our approach to generate a tailored targeted toxin called "proimmunolysin" for cancer therapy with 2-fold specificity provided by specific ligand−receptor binding and protease activation. Tumor-specific ligands, such as cancer-specific monoclonal antibodies (mAb) and growth factors might be used rather than galectin-1.

It has been reported that the binding of $\alpha$HL to hRBC is weak due to a lack of high affinity binding sites, including clustered sphingo-cholesterol domains[20] and ADAM 10.[22] The binding of $\alpha$HL to hRBC is enhanced by the fusion of galectin1 (Figure 2). We believe that the galectin-1 thereby increases the concentration of $\alpha$HL on the cell surface and thus enhances the hemolytic activity. We assumed the following pore assembly mechanism of PAM$\alpha$HLG1, which is based on the pore assembly mechanism of VCC proposed by Olson et al.[5] A monomer of PAM$\alpha$HLG1 binds to the galectin-1 receptor. MMP-2 on the proximity of the cells cleaves


DOI: 10.1021/acscentsci.8b00910
ACS Cent. Sci. 2019, 5, 629−639

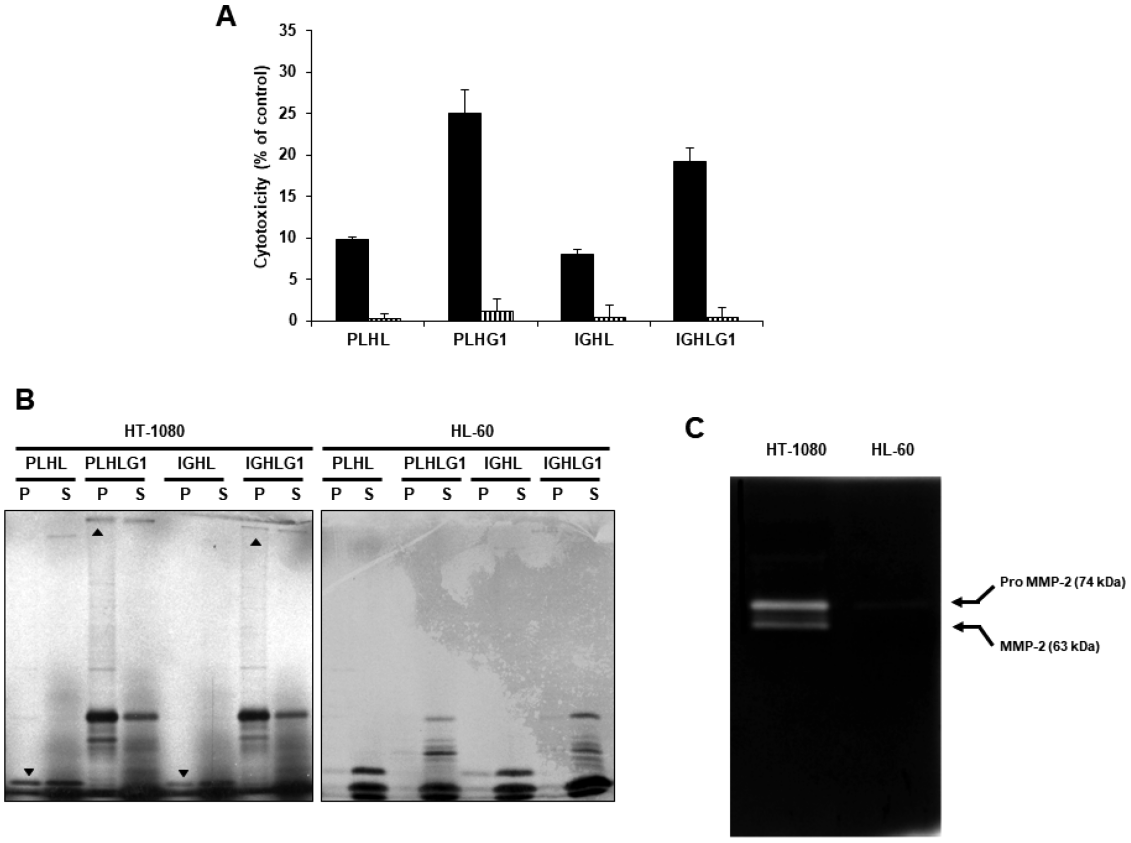


**Figure 6.** Cytotoxicity of PAMs toward cultured cancer cell lines, HT-1080 and HL-60 cells. (A) Cytotoxicity of PAMs toward HT-1080 (solid bars) or HL-60 (lined bars) cells. The cytotoxicity was evaluated by using the CytoTox 96 kit (Promega) after 8 h of incubation with PAM$\alpha$HL or PAM$\alpha$HLG1; the absorbance at 490 nm representing the concentration of released lactate dehydrogenase was recorded with a microtiter plate reader. Cytotoxicity (%) = $((A_s - A_{spon})/(A_{max} - A_{spon})) \times 100$ where $A_s$ is the absorbance of toxin-treated cells, $A_{spon}$ is the absorbance of untreated cells (spontaneously dead cells), and $A_{max}$ is the absorbance of cells treated with lysis buffer. (B) Binding assay of PAMs to HT-1080 and HL-60 cells determined by electrophoresis in a 10% SDS-polyacrylamide gel, followed by autoradiography. PAMs (PLHL, PLHLG1, IGHL, IGHLG1; 62 nM) were incubated with HT-1080 cells or HL-60 cells ($1 \times 10^7$ cells $mL^{-1}$) in 5% $CO_2$ for 40 min at 37 °C. After centrifugation, the resuspended pellets and the supernatants were analyzed. ▲, oligomers; P, pellet; S, supernatant. (C) Extent of MMP-2 expression from HT-1080 and HL-60 cells analyzed by SDS-PAGE gelatin zymography. HT-1080 cells and HL-60 cells were incubated in serum-free DMEM and IMDM, respectively, in 5% $CO_2$ at 37 °C overnight. The media were collected, centrifuged to remove debris, and mixed with zymogram sample buffer before loading into the zymogram gel (2 $\mu$g final concentration of total protein).

redundant peptides at the central loop of PAM$\alpha$HLG1 (Figure 5), and PAM$\alpha$HLG1 forms functional pores containing a nick at the central loop. However, bettter understanding of the mechanism of pore-formation by PAM$\alpha$HLG1 will be necessary to engineer $\alpha$HL for cancer therapeutics. For example, we need to know whether proteolytic activation occurs before PAM$\alpha$HLG1 binding to membranes. We believe that the two fragments of PAM$\alpha$HLG1 come together in solution because they can be ligated to each other.[24] Once they are together, the redundant peptides are removed by proteolysis, which allows assembly into a functional pore. Proteolysis might also occur when the fragments are apart, and then the complementary fragments would become active after association.

Engineered PFTs that primarily kill target cells by breaching cell membranes offer potential improvements over current targeted toxin therapies where cell entry is required. Bacterial PFTs, such as *Listeria monocytogenes* cholesterol-dependent pore-forming cytolysin (listeriolysin O),[42] and a sea anemone cytolysin,[43] have been exploited to create anticancer agents. Collier and colleagues reported that mPA-ZHER2, in which the cell-binding domain of the pore-forming component (PA) of anthrax toxin was swapped with an affibody[44] targeting HER2, showed high specificity and potency against HER2-positive cancer cells. Interestingly, mPA-ZHER2 showed cytotoxicity against a trastuzumab-resistant cell line.[13,45] Recently, bacteria that deliver pore-forming toxins, i.e., cytolysin A and $\alpha$-hemolysin, near tumors have been shown to produce therapeutic benefits.[46−48] Further, the antitumor activity of $\alpha$HL has been demonstrated in xenograft mice by killing tumor cells by necrosis.[48]

In this report, we demonstrated a potential for using engineered $\alpha$HL in cancer therapeutics. However, there is one drawback: PAM$\alpha$HL chimera bind to the native receptor of $\alpha$HL, ADAM10.[22] ADAM10 is expressed on HL-60 and HT-1080 cells, which were our target cell lines.[49,50] This explains why $\alpha$HL possessed limited cytotoxicity toward HT-1080 and HL-60 cells, but not toward hRBCs that lack ADAM 10[22] (Figures 3 and 4). To enhance the binding specificity of PAM$\alpha$HL chimera toward target cell membranes, it will be necessary to locate and ablate the ADAM10-binding site on $\alpha$HL. Additionally, a tumor-associated protease can serve an important role, as a "biological switch", in targeted cancer therapeutics such as in nanoparticles,[51] cell-penetrating


DOI: 10.1021/acscentsci.8b00910
ACS Cent. Sci. 2019, 5, 629−639

peptides,[52] liposomal drugs,[53] and prodrugs.[54] Torchilin and colleagues have claimed that a single targeting factor, such as proteinase-triggered mechanism, may not be effective due to regulated tumor proteinases in noncancerous cells.[55] Therefore, our 2-fold specificity approach utilizing dual targeting is an efficient means to attenuate toxic effects toward noncancerous cells.

We previously demonstrated that pore-formation by αHL increased the transport of trehalose into fibroblasts, which significantly increased the survival of cells during cryopreservation.[56] Recently, engineered pore-forming toxins have been developed for the delivery of therapeutic agents.[11] Pirie et al. reported that engineered cholesterol-dependent cytolysins, listeriolysin and perfringolysin, improved the delivery of immunotoxins. These toxins disrupted endosomes releasing immunotoxins into the cytoplasm, and thereby enhanced therapeutic efficacy, whereas traditional endosomal delivery systems result in the lysosomal degradation of immunotoxins.[57] These results indicate that our 2-fold specificity approach might be applied for the targeted delivery of impermeant anticancer agents.

## METHODS

**Cell Lines.** Human red blood cells were purchased from Stanford Blood Center (Palo Alto, CA). HL-60 cells were grown under 5% $CO_2$ at 37 °C in Iscove's modified Dulbecco's medium (IMDM, ThermoFisher). HT-1080 cells at 80% confluence were treated with trypsin-EDTA [0.25% (w/v) trypsin and 0.38 g $L^{-1}$ EDTA with phenol red, GIBCO] at 37 °C, under 5% $CO_2$, for 5 min, followed by the addition of FBS to inhibit trypsinization.

**Construction of αHLG1 and PAMαHLG1s.** To construct αHLG1, a modified αHL gene in a T7 vector (pT7-αHL-RL3-CTEx) was used.[18] The αHL-RL3-CTEx gene encodes the entire wild-type αHL protein (WTαHL amino acids 1−293)[18] but the gene was modified to contain six silent restriction sites (from 5′ to 3′: *SacII, HpaI, BsiWI, StuI, AflII, XhoI*) within the central region that encodes the transmembrane β-barrel of the assembled heptameric pore. Additionally, the αHL-RL3-CTEx gene carries a 3′-extension containing inverted *EarI* sites that allow for a seamless addition of coding sequences. Codon-293 of WTαHL is in bold.

```
                                  EarI      HindIII

-AATAGAAGAGGTAGTTCTGGCTCTTCCTGATAAGCTT -3′

-TTATCTTCTCCATCAAGACCAGAAAGGACTATTAGAA -5′

    EarI
```

pT7-αHL-RL3-CTEx was used to construct another extended αHL gene in the T7 vector, pT7-αHL-ESA, which encodes a flexible linker (Thr−Ser−Ser−Gly−Ser−Ser) that extends from the last codon of the WTαHL gene. Two *EarI* sites follow this linker. The 3′-extension in pT7-αHL-ESA contains restriction sites (from 5′ to 3′: *SpeI, EarI, ApaI, EarI, HindIII*) and includes a His tag-encoding sequence for metal chelate affinity purification of expressed protein (Figure S6). To construct pT7-αHL-ESA, pT7-αHL-RL3-CTEx was digested with *EarI* and *HindIII* and ligated with the following three DNA cassettes to yield pT7-αHL-ESA: cassette 1, 5′-AATACTAGTAGCGGATCGTCCAGAAGAG (sense), 5′-ACCTCTTCTGGACGATCCGCTACTAGT (antisense); cassette 2, phosphorylated 5′-GTGGGCCCGCAGCGGCTCTTCCAGTTC (sense), phosphorylated 5′-CCGAACTGGAAGAGCCGCTGCGGGCCC (antisense); and cassette 3, 5′-GGGACACCACCATCACCACCATTGATA (sense) and 5′-AGCTTATCAATGGTGGTGATGGTGGTGTC (antisense). To construct pT7-αHLG1, the human galectin-1 gene was amplified by PCR from a plasmid (pOTB7) obtained from the American Type Culture Collection (ATTC, Manassas, VA) with the following primers: 5′-AGTTACTCTTCGTCCATGGCTTGTGGTCTG GTCGC (forward) and 5′-AGTGGCGCCTACTCTTCG-ACT***TCA***GTCAAAGGCCACACATT (reverse). These primers place *EarI* sites (underlined) at the 5′ and 3′ ends of the gene, which are inverted with respect to each other. The resulting DNA fragment was digested with *EarI* and ligated into pT7-αHL-ESA that had been cut with the same enzyme to yield pT7-αHLG1. In this paper, we did not use the His tag-encoding version of the fused galectin-1 gene (i.e., αHLG1-H6). Therefore, a stop codon was included in the reverse primer (bold italics).

All protease-activatable mutants of αHLG1 (PAMαHLG1s) were constructed from pT7-αHLG1 and pT7-RR (a two-chain mutant of αHL containing a protease cleavage site, amino acid sequence: TRRI)[25] by in vitro recombination of PCR-amplified fragments[58] (Figure S1). Two plasmids were used to encode PAMαHLG1: pT7-αHL-A and pT7-αHLG1-B, which produced PAM-A (residues 1−131 of αHL) and PAMαHLG1-B (residues 119−293 of αHL, followed by a TSSGSS linker and residues 1−134 of galectin-1), respectively. pT7-RR (which contains two *HindIII* sites and two *NdeI* sites) was digested with restriction enzymes: *HindIII* to make pT7-αHL-A and with *NdeI* to make pT7-αHLG1-B (Figure S1). pT7-RR was solely digested with *HindIII*, which resulted in 'self-ligation' and form pT7-αHL-A (Figure S1). pT7-RR/*NdeI* (pT7-αHLG1-B) was further digested with *MfeI* and *SacI*, and was ligated to the double digested fragment from pT7-αHLG1/*MfeI* and *SacI* to make pT7-αHLG1-B (Figure S1). An MMP-2-recognition domain was introduced into pT7-αHLG1-B by PCR mutagenesis with the following primers: 5′-ACTGGTGATGATCCACTAGGTCTAGCCGGTG-GAGGCCTTATT-3′ (sense); 5′-AATAAGGCCTCC-ACCGGCTAGACCTAGTGGATCATCACCAGT-3′ (antisense).

**In Vitro Transcription and Translation (IVTT).** As we previously demonstrated, proteins were expressed in a cell-free coupled IVTT system by following the instruction provided by the company (Promega).[27]

The concentration of αHLG1 from an IVTT mix was calculated based on analysis of radioactive band intensities after synthesis in the presence of [$^{35}$S]methionine and electrophoresis in 10% SDS-polyacrylamide gels as previously described.[27] After electrophoresis, the gels were dried and exposed to a phosphor-imager screen (Molecular Imager Pharos FX Plus, Bio-Rad). For quantitation, the numbers of methionine residues in the polypeptides (αHL, 7; αHLG1, 9; PAM-A, 3; PAMαHL-B, 5; PAMαHLG1-B, 7) were taken into consideration as well as the known αHL concentration derived from hemolysis assay.

The ratio of the number of methionines is 1.3 (αHL:αHLG1 = 7:9): [αHL] (amount (μL) of αHL for experiment) = [αHLG1] (amount (μL) of αHLG1 for experiment) × 1.3 (band intensity of αHLG1/band intensity of αHL). To evaluate the band intensity, an equal volume of radiolabeled


DOI: 10.1021/acscentsci.8b00910
ACS Cent. Sci. 2019, 5, 629−639

IVTTs were loaded onto a 10% SDS-polyacrylamide gel. After electrophoresis, the gel was dried and exposed to the phosphor-imager screen (Kodak) for 30 min total (proper exposure duration is critical to prevent saturation). The specific radioactivity of αHLG1 was determined by using the specific activity of αHL from a hemolysis assay; $HC_{50}$ of αHL is 25 ng $mL^{-1}$.[18]

No unexpected or unusually high safety hazards were encountered. All experiments were performed at BSL2 level. However, overexpression and purification of αHLG1 may be considered a potential biohazard because αHLG1 is active toward human cells. However, we used IVTT for safety reasons, so that a human-directed pore-forming protein was not expressed in *Escherichia coli*.

**Lysis Assays.** Whole blood was washed to yield RBCs (hRBC or rRBC), which were suspended at 1% in MBSA [10 mM 3-(*N*-morpholino) propanesulfonic acid (MOPS), 150 mM NaCl, 1 mg $mL^{-1}$ bovine serum albumin (BSA), pH 7.4]. Proteins synthesized by IVTT were diluted into MBSA and subjected to 2-fold serial dilution in the same buffer in microtiter wells (50 μL final volume). RBCs (1%, 50 μL) were pipetted into each well containing the serially diluted protein to produce a final assay volume of 100 μL. Hemolysis was recorded by monitoring the decreases in light scattering at 595 nm. For long-duration hemolysis assays, the microtiter plate was covered with an adhesive film to prevent evaporation between measurements and stored at room temperature. The optical density (OD) at 595 nm was monitored at 10 different time points up to 72 h (TECAN). The presented results are the average of three experimental sets ($n$ = 3). The percent of cells lysed at a time ($t$) was calculated: % cell lysis = $((OD_{initial} - OD_t)/(OD_{initial} - OD_{final})) \times 100$, where $OD_{initial}$, $OD_{final}$, and $OD_t$ are the initial and final ODs, and the OD at time $t$, respectively. The initial lag period was taken to be the time at which 10% lysis had occurred. The hemolysis rate (% cells lysed $s^{-1}$) was derived from the time required to reach ∼80% lysis. HL-60 cells were washed twice with PBS and resuspended in IMDM containing 3% FBS. The cells were then divided into three tubes (polystyrene round-bottom tube, Falcon): control, αHL, and αHLG1. The lysis of HL-60 cells ($1 \times 10^7$ cells $mL^{-1}$) was monitored by flow cytometry (FACSCalibur, Becton Dickinson) every 5 min for 75 min after the addition of the toxin. The sample tubes were gently agitated during the incubation. Forward scatter (FSC) and side scatter (SSC) were monitored to identify damaged cells and cell debris. Data analysis was performed by Cellquest (BectonDickinson, Franklin Lakes, NJ) (Figure S5). Percent lysis (%) = $((N_s - N_c)/(N_t - N_c)) \times 100$, where $N_s$ is the number of lysed cells in the treated sample, $N_c$ is the number of lysed cells in the untreated control sample, and $N_t$ is total number of cells in the assay ($N_t$ = 10 000). The results are presented as the means of three independent assays ($n$ = 3, with triplicate reads in each).

**Inhibition of αHLG1 Activity by Carbohydrates.** To examine hemolysis inhibition, αHLG1 was mixed with MBSA containing various carbohydrates and incubated for 20 min at room temperature before 2-fold serial dilution across a row of a 96-well microtiter plate. Hemolysis of 0.5% RBCs was monitored by observing the decrease in light scattering at 595 nm for 1 h. The inhibition of membrane binding by carbohydrates was performed by incubating $^{35}S$-labeled αHLG1 made by IVTT with the assay buffer (MBSA and carbohydrates) for 20 min before the addition of washed RBCs in MBSA to a final concentration of 0.5%. The assay mix (αHLG1, 20 nM final) was incubated for 30 min and centrifuged. The supernatant and resuspended pellet were loaded onto 10% SDS-polyacrylamide gels. After electrophoresis, dried gels were subjected to autoradiography.

**Binding Assay.** IVTT proteins were added to the cells (20 μL of 0.5% RBCs, 30 μL of HL-60 cells or HT-1080 cells at $1 \times 10^7$ cells $mL^{-1}$) and incubated for 20 min (RBCs) or 40 min (HL-60 and HT-1080 cells) at room temperature. The cells were recovered by centrifugation for 3 min at 12000*g*. For the HL-60 or HT-1080 cells, cell pellets (18 μL) were resuspended in MBSA and treated with 2 μL of DNase (2000 units $mL^{-1}$, New England Biolabs) for 30 min at 37 °C. The cells were then pelleted and washed with MBSA twice. After centrifugation, the pellets and supernatants were dissolved in 2× loading buffer without heating, and separated in a 10% SDS-polyacrylamide gel. Autoradiography was carried out as detailed above. To examine the binding of PAM (protease-activatable mutants), PAMs were incubated with HL-60 or HT-1080 cells ($1 \times 10^7$ cells $mL^{-1}$) for 40 min at 37 °C under 5% $CO_2$.

**Activation of PAMs by Proteolysis.** Cathepsin B (Calbiochem) was first activated in 50 mM sodium acetate, 15 mM EDTA, and 30 mM dithiothreitol at pH 5.9, for 30 min at 37 °C. PAMs were then treated with the activated cathepsin B (0.8 μg $\mu L^{-1}$) for 40 min at 37 °C, followed by inactivation with leupeptin (1 mM). Procedures for proenzyme activation and MMP-2 storage were as described by the manufacturer (Calbiochem). The proenzyme (as supplied) was mixed 10:1 (v/v) with 30 mM aminophenylmercuric acetate (APMA) in 0.1 M NaOH (Sigma-Aldrich) and incubated for 2 h at 37 °C prior to storage in 50 mM Tris-HCl, pH 7.6, 5 mM $CaCl_2$, and 20% glycerol at −80 °C. Activated MMP-2 (0.3 μg $\mu L^{-1}$ final) was incubated with PAMs for 40 min at 37 °C and inhibited by adding 1.25 mM MMP-2 inhibitor I (*cis*-9-octadecenoyl-*N*-hydroxylamide, Calbiochem). PAMαHLG1 (36 nM) was incubated at 37 °C for 30 min with MMP-2 (0.3 μg $\mu L^{-1}$) or cathepsin B (0.8 μg $\mu L^{-1}$).

**Cytotoxicity Assay.** HT-1080 cells were cultured to 80% confluence and trypsinized as detailed previously. The harvested HT-1080 cells were resuspended in DMEM (10% FBS), and HL-60 cell pellets were resuspended with IMDM (20% FBS). The cells were then seeded onto uncoated 96-well tissue-culture plates (Falcon) and incubated for 16 h (80% confluence, HT-1080 cells). The medium was then removed from the wells, and the cells were washed twice with PBS. Toxins in medium including 3% FBS were added to each well and incubated for different time periods (HL-60 cells, 75 min for αHL and αHLG1, 8 h for PAMs; HT-1080 cells, 2 h for αHL and αHLG1, 8 h for PAMs) under 5% $CO_2$ at 37 °C. The cytotoxicities toward HL-60 and HT-1080 cells were measured by determining lactate dehydrogenase (LDH) activity released upon cell lysis (CytoTox 96 Assay, Promega), by measuring absorbance at 490 nm with a microplate reader and the Magellan management program (both from TECAN). Percent cytotoxicity is defined as cytotoxicity (%) = $((A_s - A_{spon})/(A_{max} - A_{spon})) \times 100$, where $A_s$ is absorbance from the LDH assay (cells treated with toxin), $A_{spon}$ is absorbance from untreated cells, and $A_{max}$ is absorbance from fully lysed cells.

**Gelatin Zymography.** MMP-2 enzymatic activity in tissue culture media was determined by 10% SDS-PAGE gelatin zymography (Ready Gel Zymogram Gel, Bio-Rad). HT-1080 cells and HL-60 cells in serum-free media were incubated at


DOI: 10.1021/acscentsci.8b00910
ACS Cent. Sci. 2019, 5, 629−639

5% $CO_2$ at 37 °C for 18 h. Media were gently collected by pipetting and centrifuged for 5 min to remove debris and floating cells. Total protein concentration in the clear media was measured and equal amounts of proteins (2 μg, final) were loaded in each lane of the SDS-PAGE gelatin zymogram gel. Before electrophoresis media were mixed with the zymogram sample buffer (62.5 mM Tris-HCl, 4% SDS, 25% glycerol, 0.01% Bromophenol Blue, Bio-Rad). After electrophoresis, the gel was incubated in renaturing solution (2.5% Triton X-100) for 30 min with gentle agitation, incubated in development solution (50 mM Tris, 200 mM NaCl, 5 mM $CaCl_2$, 0.02% Brij-35, pH 7.5, Bio-Rad) at 37 °C overnight, stained with 0.5% Coomassie blue R-250 for 1 h, and destained with destaining solution (40% methanol and 10% acetic acid).

## ■ ASSOCIATED CONTENT

### Supporting Information

The Supporting Information is available free of charge on the ACS Publications website at DOI: 10.1021/acscentsci.8b00910.

Binding efficacy of toxins, sequence of protease-recognition domain, description of construction of PAMαHL and PAMαHLG1 with pT7 vector, hemolysis assay, inhibition assay, binding assay, raw data of lysis assay, and DNA sequence of pT7αHL-CTEx-ESA for construction of αHLG1 (PDF)

## ■ AUTHOR INFORMATION


### Corresponding Authors

*E-mail: swkoo@tamu.edu. Phone: 1-979-436-0381.

*E-mail: hagan.bayley@chem.ox.ac.uk. Phone: +44 1865 285101.

### ORCID

Sunwoo Koo: 0000-0003-2715-909X

Hagan Bayley: 0000-0003-2499-6116


### Notes

The authors declare no competing financial interest.

## ■ ACKNOWLEDGMENTS

This work was supported by grants (Hagan Bayley) from the U.S. Department of Energy, the National Institutes of Health, the Office of Naval Research (MURI-1999), and the Texas Advanced Technology Program.

## ■ DEDICATION

‖This paper is dedicated to the memory of our wonderful colleague, Dr. Stephen Cheley, who passed away.

## ■ REFERENCES


(1) Bayley, H.; Jayasinghe, L. Functional engineered channels and pores (Review). *Mol. Membr. Biol.* **2004**, *21* (4), 209.

(2) Ayub, M.; Bayley, H. Engineered transmembrane pores. *Curr. Opin. Chem. Biol.* **2016**, *34*, 117.

(3) Iacovache, I.; Paumard, P.; Scheib, H.; Lesieur, C.; Sakai, N.; Matile, S.; Parker, M. W.; van der Goot, F. G. A rivet model for channel formation by aerolysin-like pore-forming toxins. *EMBO J.* **2006**, *25* (3), 457.

(4) Miller, C. J.; Elliott, J. L.; Collier, R. J. Anthrax protective antigen: prepore-to-pore conversion. *Biochemistry* **1999**, *38* (32), 10432.

(5) Olson, R.; Gouaux, E. Crystal structure of the Vibrio cholerae cytolysin (VCC) pro-toxin and its assembly into a heptameric transmembrane pore. *J. Mol. Biol.* **2005**, *350* (5), 997.

(6) Walker, B.; Krishnasastry, M.; Zorn, L.; Bayley, H. Assembly of the oligomeric membrane pore formed by Staphylococcal alpha-hemolysin examined by truncation mutagenesis. *J. Biol. Chem.* **1992**, *267* (30), 21782−21786.

(7) Bhakdi, S.; Tranum-Jensen, J. Alpha-toxin of Staphylococcus aureus. *Microbiol Rev.* **1991**, *55* (4), 733−751.

(8) Abrami, L.; Fivaz, M.; Decroly, E.; Seidah, N. G.; Jean, F.; Thomas, G.; Leppla, S. H.; Buckley, J. T.; van der Goot, F. G. The pore-forming toxin proaerolysin is activated by furin. *J. Biol. Chem.* **1998**, *273* (49), 32656.

(9) Gordon, V. M.; Klimpel, K. R.; Arora, N.; Henderson, M. A.; Leppla, S. H. Proteolytic activation of bacterial toxins by eukaryotic cells is performed by furin and by additional cellular proteases. *Infect. Immun.* **1995**, *63* (1), 82−87.

(10) Valeva, A.; Walev, I.; Weis, S.; Boukhallouk, F.; Wassenaar, T. M.; Endres, K.; Fahrenholz, F.; Bhakdi, S.; Zitzer, A. A cellular metalloproteinase activates Vibrio cholerae pro-cytolysin. *J. Biol. Chem.* **2004**, *279* (24), 25143.

(11) Gurnev, P. A.; Nestorovich, E. M. Channel-forming bacterial toxins in biosensing and macromolecule delivery. *Toxins* **2014**, *6* (8), 2483.

(12) Qiu, X. Q.; Wang, H.; Lu, X. F.; Zhang, J.; Li, S. F.; Cheng, G.; Wan, L.; Yang, L.; Zuo, J. Y.; Zhou, Y. Q.; et al. An engineered multidomain bactericidal peptide as a model for targeted antibiotics against specific bacteria. *Nat. Biotechnol.* **2003**, *21* (12), 1480.

(13) Mechaly, A.; McCluskey, A. J.; Collier, R. J. Changing the receptor specificity of anthrax toxin. *mBio* **2012**, *3* (3), e00088−12.

(14) Liu, S.; Liu, J.; Ma, Q.; Cao, L.; Fattah, R. J.; Yu, Z.; Bugge, T. H.; Finkel, T.; Leppla, S. H. Solid tumor therapy by selectively targeting stromal endothelial cells. *Proc. Natl. Acad. Sci. U. S. A.* **2016**, *113* (28), No. E4079.

(15) Liu, S.; Redeye, V.; Kuremsky, J. G.; Kuhnen, M.; Molinolo, A.; Bugge, T. H.; Leppla, S. H. Intermolecular complementation achieves high-specificity tumor targeting by anthrax toxin. *Nat. Biotechnol.* **2005**, *23* (6), 725.

(16) Jayasinghe, L.; Miles, G.; Bayley, H. Role of the amino latch of staphylococcal alpha-hemolysin in pore formation: a co-operative interaction between the N terminus and position 217. *J. Biol. Chem.* **2006**, *281* (4), 2195.

(17) Walker, B.; Bayley, H. Key residues for membrane binding, oligomerization, and pore forming activity of staphylococcal alpha-hemolysin identified by cysteine scanning mutagenesis and targeted chemical modification. *J. Biol. Chem.* **1995**, *270* (39), 23065.

(18) Walker, B.; Krishnasastry, M.; Zorn, L.; Kasianowicz, J.; Bayley, H. Functional expression of the alpha-hemolysin of Staphylococcus aureus in intact Escherichia coli and in cell lysates. Deletion of five C-terminal amino acids selectively impairs hemolytic activity. *J. Biol. Chem.* **1992**, *267* (15), 10902−10909.

(19) Hildebrand, A.; Pohl, M.; Bhakdi, S. Staphylococcus aureus alpha-toxin. Dual mechanism of binding to target cells. *J. Biol. Chem.* **1991**, *266* (26), 17195−17200.

(20) Valeva, A.; Hellmann, N.; Walev, I.; Strand, D.; Plate, M.; Boukhallouk, F.; Brack, A.; Hanada, K.; Decker, H.; Bhakdi, S. Evidence that clustered phosphocholine head groups serve as sites for binding and assembly of an oligomeric protein pore. *J. Biol. Chem.* **2006**, *281* (36), 26014.

(21) Galdiero, S.; Gouaux, E. High resolution crystallographic studies of alpha-hemolysin-phospholipid complexes define heptamer-lipid head group interactions: implication for understanding protein-lipid interactions. *Protein Sci.* **2004**, *13* (6), 1503.

(22) Wilke, G. A.; Bubeck Wardenburg, J. Role of a disintegrin and metalloprotease 10 in Staphylococcus aureus alpha-hemolysin-mediated cellular injury. *Proc. Natl. Acad. Sci. U. S. A.* **2010**, *107* (30), 13473.

(23) Walker, B.; Krishnasastry, M.; Bayley, H. Functional complementation of staphylococcal alpha-hemolysin fragments.

Overlaps, nicks, and gaps in the glycine-rich loop. *J. Biol. Chem.* **1993**, *268* (7), 5285−5292.
(24) Walker, B.; Bayley, H. A pore-forming protein with a protease-activated trigger. *Protein Eng., Des. Sel.* **1994**, *7* (1), 91.
(25) Panchal, R. G.; Cusack, E.; Cheley, S.; Bayley, H. Tumor protease-activated, pore-forming toxins from a combinatorial library. *Nat. Biotechnol.* **1996**, *14* (7), 852.
(26) Rai, A. K.; Paul, K.; Chattopadhyay, K. Functional mapping of the lectin activity site on the beta-prism domain of vibrio cholerae cytolysin: implications for the membrane pore-formation mechanism of the toxin. *J. Biol. Chem.* **2013**, *288* (3), 1665.
(27) Miles, G.; Bayley, H.; Cheley, S. Properties of Bacillus cereus hemolysin II: a heptameric transmembrane pore. *Protein Sci.* **2002**, *11* (7), 1813.
(28) Hammerstein, A. F.; Jayasinghe, L.; Bayley, H. Subunit dimers of alpha-hemolysin expand the engineering toolbox for protein nanopores. *J. Biol. Chem.* **2011**, *286* (16), 14324.
(29) Timoshenko, A. V.; Gorudko, I. V.; Maslakova, O. V.; Andre, S.; Kuwabara, I.; Liu, F. T.; Kaltner, H.; Gabius, H. J. Analysis of selected blood and immune cell responses to carbohydrate-dependent surface binding of proto- and chimera-type galectins. *Mol. Cell. Biochem.* **2003**, *250* (1−2), 139.
(30) Dias-Baruffi, M.; Zhu, H.; Cho, M.; Karmakar, S.; McEver, R. P.; Cummings, R. D. Dimeric galectin-1 induces surface exposure of phosphatidylserine and phagocytic recognition of leukocytes without inducing apoptosis. *J. Biol. Chem.* **2003**, *278* (42), 41282.
(31) Sorme, P.; Kahl-Knutsson, B.; Wellmar, U.; Magnusson, B. G.; Leffler, H.; Nilsson, U. J. Design and synthesis of galectin inhibitors. *Methods Enzymol.* **2003**, *363*, 157.
(32) Guo, H. B.; Lee, I.; Kamar, M.; Pierce, M. N-acetylglucosaminyltransferase V expression levels regulate cadherin-associated homotypic cell-cell adhesion and intracellular signaling pathways. *J. Biol. Chem.* **2003**, *278* (52), 52412.
(33) Janowska-Wieczorek, A.; Marquez, L. A.; Matsuzaki, A.; Hashmi, H. R.; Larratt, L. M.; Boshkov, L. M.; Turner, A. R.; Zhang, M. C.; Edwards, D. R.; Kossakowska, A. E. Expression of matrix metalloproteinases (MMP-2 and −9) and tissue inhibitors of metalloproteinases (TIMP-1 and −2) in acute myelogenous leukaemia blasts: comparison with normal bone marrow cells. *Br. J. Haematol.* **1999**, *105* (2), 402.
(34) Seltzer, J. L.; Akers, K. T.; Weingarten, H.; Grant, G. A.; McCourt, D. W.; Eisen, A. Z. Cleavage specificity of human skin type IV collagenase (gelatinase). Identification of cleavage sites in type I gelatin, with confirmation using synthetic peptides. *J. Biol. Chem.* **1990**, *265* (33), 20409−20413.
(35) Roshy, S.; Sloane, B. F.; Moin, K. Pericellular cathepsin B and malignant progression. *Cancer Metastasis Rev.* **2003**, *22* (2−3), 271.
(36) Chen, E. I.; Kridel, S. J.; Howard, E. W.; Li, W.; Godzik, A.; Smith, J. W. A unique substrate recognition profile for matrix metalloproteinase-2. *J. Biol. Chem.* **2002**, *277* (6), 4485.
(37) Maquoi, E.; Noel, A.; Frankenne, F.; Angliker, H.; Murphy, G.; Foidart, J. M. Inhibition of matrix metalloproteinase 2 maturation and HT1080 invasiveness by a synthetic furin inhibitor. *FEBS Lett.* **1998**, *424* (3), 262.
(38) Hulkower, K. I.; Butler, C. C.; Linebaugh, B. E.; Klaus, J. L.; Keppler, D.; Giranda, V. L.; Sloane, B. F. Fluorescent microplate assay for cancer cell-associated cathepsin B. *Eur. J. Biochem.* **2000**, *267* (13), 4165.
(39) Berquin, I. M.; Yan, S.; Katiyar, K.; Huang, L.; Sloane, B. F.; Troen, B. R. Differentiating agents regulate cathepsin B gene expression in HL-60 cells. *J. Leukocyte Biol.* **1999**, *66* (4), 609.
(40) Stowell, S. R.; Dias-Baruffi, M.; Penttila, L.; Renkonen, O.; Nyame, A. K.; Cummings, R. D. Human galectin-1 recognition of poly-N-acetyllactosamine and chimeric polysaccharides. *Glycobiology* **2003**, *14* (2), 157.
(41) Yemul, S.; Berger, C.; Estabrook, A.; Suarez, S.; Edelson, R.; Bayley, H. Selective killing of T lymphocytes by phototoxic liposomes. *Proc. Natl. Acad. Sci. U. S. A.* **1987**, *84* (1), 246.
(42) Bergelt, S.; Frost, S.; Lilie, H. Listeriolysin O as cytotoxic component of an immunotoxin. *Protein Sci.* **2009**, *18* (6), 1210.
(43) Tejuca, M.; Diaz, I.; Figueredo, R.; Roque, L.; Pazos, F.; Martinez, D.; Iznaga-Escobar, N.; Perez, R.; Alvarez, C.; Lanio, M. E. Construction of an immunotoxin with the pore forming protein StI and ior C5, a monoclonal antibody against a colon cancer cell line. *Int. Immunopharmacol.* **2004**, *4* (6), 731.
(44) Wahlberg, E.; Lendel, C.; Helgstrand, M.; Allard, P.; Dincbas-Renqvist, V.; Hedqvist, A.; Berglund, H.; Nygren, P. A.; Hard, T. An affibody in complex with a target protein: structure and coupled folding. *Proc. Natl. Acad. Sci. U. S. A.* **2003**, *100* (6), 3185.
(45) McCluskey, A. J.; Olive, A. J.; Starnbach, M. N.; Collier, R. J. Targeting HER2-positive cancer cells with receptor-redirected anthrax protective antigen. *Mol. Oncol.* **2013**, *7* (3), 440.
(46) Jiang, S. N.; Phan, T. X.; Nam, T. K.; Nguyen, V. H.; Kim, H. S.; Bom, H. S.; Choy, H. E.; Hong, Y.; Min, J. J. Inhibition of tumor growth and metastasis by a combination of Escherichia coli-mediated cytolytic therapy and radiotherapy. *Mol. Ther.* **2010**, *18* (3), 635.
(47) Swofford, C. A.; St Jean, A. T.; Panteli, J. T.; Brentzel, Z. J.; Forbes, N. S. Identification of Staphylococcus aureus alpha-hemolysin as a protein drug that is secreted by anticancer bacteria and rapidly kills cancer cells. *Biotechnol. Bioeng.* **2014**, *111* (6), 1233.
(48) St Jean, A. T.; Swofford, C. A.; Panteli, J. T.; Brentzel, Z. J.; Forbes, N. S. Bacterial delivery of Staphylococcus aureus alpha-hemolysin causes regression and necrosis in murine tumors. *Mol. Ther.* **2014**, *22* (7), 1266.
(49) Wu, E.; Croucher, P. I.; McKie, N. Expression of members of the novel membrane linked metalloproteinase family ADAM in cells derived from a range of haematological malignancies. *Biochem. Biophys. Res. Commun.* **1997**, *235* (2), 437.
(50) Xu, D.; Sharma, C.; Hemler, M. E. Tetraspanin12 regulates ADAM10-dependent cleavage of amyloid precursor protein. *FASEB J.* **2009**, *23* (11), 3674.
(51) Zhu, L.; Perche, F.; Wang, T.; Torchilin, V. P. Matrix metalloproteinase 2-sensitive multifunctional polymeric micelles for tumor-specific co-delivery of siRNA and hydrophobic drugs. *Biomaterials* **2014**, *35* (13), 4213.
(52) LeBeau, A. M.; Denmeade, S. R. Protease-Activated Pore-Forming Peptides for the Treatment and Imaging of Prostate Cancer. *Mol. Cancer Ther.* **2015**, *14*, 659.
(53) Basel, M. T.; Shrestha, T. B.; Troyer, D. L.; Bossmann, S. H. Protease-sensitive, polymer-caged liposomes: a method for making highly targeted liposomes using triggered release. *ACS Nano* **2011**, *5* (3), 2162.
(54) Alfano, R. W.; Leppla, S. H.; Liu, S.; Bugge, T. H.; Herlyn, M.; Smalley, K. S.; Bromberg-White, J. L.; Duesbery, N. S.; Frankel, A. E. Cytotoxicity of the matrix metalloproteinase-activated anthrax lethal toxin is dependent on gelatinase expression and B-RAF status in human melanoma cells. *Mol. Cancer Ther.* **2008**, *7* (5), 1218.
(55) Zhu, L.; Torchilin, V. P. Stimulus-responsive nanopreparations for tumor targeting. *Integrative biology: quantitative biosciences from nano to macro* **2013**, *5* (1), 96.
(56) Eroglu, A.; Russo, M. J.; Bieganski, R.; Fowler, A.; Cheley, S.; Bayley, H.; Toner, M. Intracellular trehalose improves the survival of cryopreserved mammalian cells. *Nat. Biotechnol.* **2000**, *18* (2), 163.
(57) Pirie, C. M.; Liu, D. V.; Wittrup, K. D. Targeted cytolysins synergistically potentiate cytoplasmic delivery of gelonin immunotoxin. *Mol. Cancer Ther.* **2013**, *12* (9), 1774.
(58) Howorka, S.; Bayley, H. Improved protocol for high-throughput cysteine scanning mutagenesis. *BioTechniques* **1998**, *25* (5), 764.


DOI: 10.1021/acscentsci.8b00910
*ACS Cent. Sci.* 2019, 5, 629−639